Structural Mechanisms of Bile Salt-Induced Growth of Small Unilamellar Cholesterol−Lecithin Vesicles†

Andrew S. Luk,‡ Eric W. Kaler,*,‡ and Sum P. Lee§

Center for Molecular and Engineering Thermodynamics, Department of Chemical Engineering, University of Delaware, Newark, Delaware 19716, and VA Medical Center, Seattle, Washington 98108

Received September 16, 1996; Revised Manuscript Received March 5, 1997⊗

ABSTRACT: The liver secretes cholesterol and lecithin in the form of mixed vesicles during the formation of bile. When exposed to bile salts, these metastable vesicles undergo various structural rearrangements. We have examined the effects of three different bile salts, taurocholate (TC), tauroursodeoxycholate (TUDC), and taurodeoxycholate (TDC), on the stability of sonicated lecithin vesicles containing various amounts of cholesterol. Vesicle growth was probed by turbidity measurements, quasi-elastic light scattering, and a resonance energy transfer lipid-mixing assay. Leakage of internal contents was monitored by encapsulation of fluorescence probes in vesicles. At low bile salt-to-lecithin ratios (TC/L or TUDC/L < 1), pure lecithin vesicles do not grow, but exhibit slow intervesicular mixing of lipids as well as gradual leakage. At high BS/L (TC/L or TUDC/L > 5), pure lecithin vesicles are solubilized into mixed micelles with a concomitant decrease in the overall particle size. In this regime, extensive leakage and lipid mixing occur instantaneously after exposure to bile salt. At intermediate BS/L (1 < TC/L or TUDC/L < 5), vesicles grow with time, and the rates of both leakage and lipid mixing are rapid. The data suggest that vesicles grow by the transfer of lecithin and cholesterol via diffusion in the aqueous medium. The addition of cholesterol to lecithin vesicles reduces leakage dramatically and increases the amount of BS required for complete solubilization of vesicles. The more hydrophobic TDC induces vesicle growth at a lower BS/L than does TC or TUDC. These results demonstrate the physiologic forms of lipid microstructures during bile formation and explain how the hydrophilic−hydrophobic balance of BS mixtures may profoundly affect the early stages of CH gallstone formation.

Bile is a complex biological fluid with four major components: bile salt (BS),[1] lecithin (L), cholesterol (CH), and water (Cabral & Small, 1989). Since the physicochemical properties of bile are relevant to the development of some liver diseases, the various phase equilibria of a model biliary lipid system have been systematically studied (Small et al., 1966; Bourgès et al., 1967a,b). Typical solute concentrations of liver and gallbladder bile are about 3 g/dL and 10 g/dL, respectively (Lee & Sekijima, 1991), and these physiological concentrations lie in the water-rich corner of the equilibrium BS−L−H_2O phase diagram as in Figure 1 (Small et al., 1966). At low BS content, multilamellar liquid crystals coexist with BS monomers (region A), and a single isotropic micellar phase forms at high BS concentrations (region D).

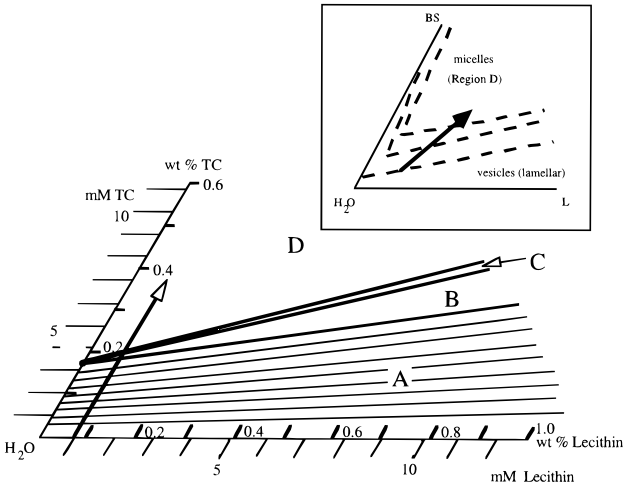

FIGURE 1: Water-rich corner of the equilibrium BS−L−H_2O phase diagram. Region A represents a two-phase region composed of a lamellar phase and an aqueous phase. Region B contains the above two phases and the hexagonal phase. Region C is a two-phase region composed of an isotropic micellar phase and a hexagonal phase, and region D is the single isotropic micellar phase. The experimental course of vesicle solubilization explored in this study is shown by the unlabeled open-head arrow [redrawn with permission from the *Handbook of Physiology* (1989)]. The inset shows schematically how the micellar region D shrinks with increasing CH content in bile (the dark arrow represents the changes with increasing amount of CH).

Neutron scattering studies on dilute model bile show that BS−L mixed micelles are rodlike or wormlike (Hjelm et al., 1992; Long et al., 1994a; Pedersen et al., 1995) and lengthen as the micellar boundary is approached (Nichols & Ozarowski, 1990; Long et al., 1994b).

† Supported in part by the Whitaker Foundation and by a Grant (DK-41678) from the National Institutes of Health. S.P.L. is supported in part by the Medical Research Service of the Department of Veterans Affairs.

* Author to whom correspondence should be addressed.

‡ Department of Chemical Engineering, University of Delaware.

§ VA Medical Center, Seattle.

⊗ Abstract published in *Advance ACS Abstracts,* April, 15, 1997.

[1] Abbreviations: CH, cholesterol; L, egg lecithin; BS, bile salt; TC, sodium taurocholate; TDC, sodium taurodeoxycholate; TUDC, sodium tauroursodeoxycholate; ANTS, 8-aminonaphthalene-1,3,6-trisulfonic acid; DPX, *p*-xylylenebis(pyridinium bromide); NBD-PE, *N*-(7-nitro-2,1,3-benzoxadiazol-4-yl)-1,2-dihexadecanoylphosphatidylethanolamine; Rh-PE, *N*-(lissamine rhodamine B sulfonyl)-1,2-dihexadecanoylphosphatidylethanolamine; SUV, small unilamellar vesicle(s); LUV, large unilamellar vesicle(s); $[BS]_{aqueous}$, aqueous BS concentration; BS/L, bile salt-to-lecithin ratio; R_e, "effective" or aggregate bile salt-to-lecithin ratio; CH/L, cholesterol-to-lecithin ratio; QELS, quasi-elastic light scattering; CMC, critical micelle concentration; IMC, intermicellar concentration; IVC, intervesicular concentration; R_h, mean hydrodynamic radius; PI, polydispersity index.

S0006-2960(96)02332-X CCC: $14.00

The BS−L−H_2O phase diagram changes upon the incorporation of CH. With increasing CH content, the single isotropic micellar region D shrinks and ultimately vanishes at above 4 wt % CH (Bourgès et al., 1967b). The isotropic micellar zone also diminishes with decreasing total lipid concentration, temperature, and the CH solubilizing capacity of the BS species (Carey & Small, 1978; Salvioli et al., 1983). Once the micellar solubility is surpassed, CH crystals appear as additional equilibrium phases (Bourgès et al., 1967b). Clinical studies demonstrate that most of the biles collected from gallstone patients have CH contents that exceed the micellar solubility of CH and are thus supersaturated (Admirand & Small, 1968).

It is believed that cholesterol and lecithin are cosecreted by liver cells in the form of thermodynamically metastable unilamellar vesicles, while the amphiphilic BS is released independently via a separate pathway (Lee et al., 1987; Cohen et al., 1989). These secreted vesicles are then partially solubilized by BS to form mixed micelles, with a concomitant increase in CH/L of the residual vesicles (Cohen et al., 1990). In addition, water is absorbed from bile during its passage to the gallbladder, and this concentrating effect further drives the transformation of vesicles to micelles (Mazer & Carey, 1983). The remaining highly metastable CH-enriched vesicles become the primary carriers for excess CH in supersaturated bile (Mazer & Carey, 1983; Sömjen & Gilat, 1985; Lee et al., 1987).

Aggregation and fusion of CH-enriched vesicles have been postulated as the precursors to cholesterol precipitation in bile (Halpern et al., 1986). On the basis of polarizing microscopy observations, a number of proteins isolated from human bile accelerate the overall CH crystallization process (Lee & Sekijima, 1991) and induce aggregation and fusion of CH−L vesicles (Luk et al., 1993, 1995). Despite extensive research aimed at identifying pro-nucleating proteins in bile and examining the final physical states of lipid aggregates formed through different equilibration pathways (Mazer & Carey, 1983; Mazer et al., 1984; Schurtenberger et al., 1985, 1986), few studies have characterized the physiological importance of BS-induced vesicle growth in the pathogenesis of cholesterol gallstone formation. Most, if not all, studies on bile salt−vesicle interaction are confined to the use of pure lecithin vesicles.

Human bile contains a number of different BS species. Bile salts are surfactants with an atypical planar polarity (Figure 2). The hydrophilic face can contain up to three hydroxyl groups, together with the terminal carboxyl group on the five-carbon side chain, while the hydrocarbon steroid backbone forms the hydrophobic face. Depending on the relative ratio of BS and lecithin, bile salts induce various structural alterations of lecithin vesicles. Cryo-transmission electron micrographs of samples containing increasing amounts of the unconjugated bile salt cholate show that vesicle-to-micelle transitions proceed through several intermediate microstructures. The morphology evolves from open vesicles to lamellar fragments to long cylindrical mixed micelles to ultimately globular micelles (Walter et al., 1991). In addition, bile salts also cause an increase in the sizes of small unilamellar lecithin vesicles (Almog & Lichtenberg, 1988; Little et al., 1991). The mechanism of such size growth, such as via either vesicle aggregation and fusion or intervesicular lipid transfer, is still under debate (Almog et al., 1986; Edwards & Almgren, 1992), and no definitive proofs are available.

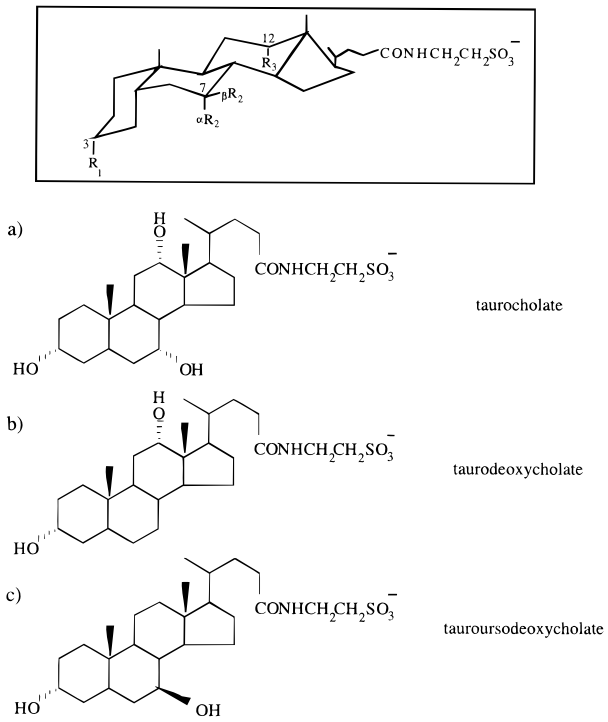

FIGURE 2: Structural formulas of the bile salts used in this study. (a) 3α,7α,12α-Taurocholate; (b) 3α,12α-taurodeoxycholate; (c) 3α,7*β*-tauroursodeoxycholate. Note that all the α-hydroxyl groups lie on the same side of the bile salt molecule.

Because of the unique surface properties of BS and their physiological roles in CH solubilization, we examine here the effects of three different taurine-conjugated bile salts, namely, taurocholate, taurodeoxycholate, and tauroursodeoxycholate, on the mechanisms of BS-induced growth of lecithin vesicles containing different amounts of CH. After the exposure of varying amounts of BS to CH−L vesicles, vesicle growth was probed qualitatively by turbidity measurements, and the changes in vesicle sizes were monitored by quasi-elastic light scattering. Vesicle leakage was followed by coencapsulating in the vesicles a pair of fluorescence probes, ANTS and DPX (Ellens et al., 1985). Leakage, and the subsequent dilution, of these probes into the external aqueous medium increases ANTS fluorescence (via dequenching). In order to elucidate the structural mechanisms of vesicle growth, small amounts of the fluorescence lipids, NBD-PE and Rh-PE, are incorporated into a population of "labeled" vesicles (Struck et al., 1981). During vesicle growth, the dilution of these lipids into "unlabeled" vesicles, either by vesicle fusion or by intervesicular transfer, will lower the efficiency of energy transfer between these probes, resulting in a change in fluorescence intensity. Sonicated unilamellar vesicles, the smallest form of the lamellar liquid crystalline phase, were employed to mimic freshly secreted biliary vesicles. This study contributes to further understanding of BS−lipid interactions and provides additional insights into the mechanistic features of the early stages of bile equilibration.

MATERIALS AND METHODS

Sodium taurocholate (TC) and sodium tauroursodeoxycholate (TUDC), all of highest purity (>99.5%), were

purchased from CalBiochem (La Jolla, CA) and used as received. Sodium taurodeoxycholate (TDC) was obtained from CalBiochem and was further purified by crystallization. Cholesterol (CH) and egg yolk lecithin (L) were obtained from Sigma (analytical grade; St. Louis, MO) and used without further purification. 8-Aminonaphthalene-1,3,6-trisulfonic acid (ANTS), *p*-xylylenebis(pyridinium bromide) (DPX), *N*-(7-nitro-2,1,3-benzoxadiazol-4-yl)phosphoethanolamine (NBD-PE), and *N*-(lissamine rhodamine B sulfonyl)phosphoethanolamine (Rh-PE) were purchased from Molecular Probes (Eugene, OR). Water used was distilled and deionized, and all glassware was acid-washed.

Small unilamellar vesicles composed of CH and L or of L alone were prepared by ultrasonication. Mixtures of CH and L were coprecipitated from chloroform in various molar ratios (approximately 0, 20, and 36 mol % CH). For the lipid-mixing assay, 0.6 mol % of each NBD-PE and Rh-PE was included in the lipid mixture. The solvent was evaporated by a stream of nitrogen in a rotary evaporator, and the residual solvent was eliminated thoroughly under vacuum. The dried lipid was resuspended in the appropriate buffer to yield a lipid concentration of 20 mg/mL. The hydrated lipid solutions were sparged with argon and directly sonicated (Heat Systems Ultrasonics Model W-225) in an ice−water bath for 90 min. Sonicated dispersions were centrifuged at 25 °C for 2 h at 32000*g*, and the top three-fourths of the supernatant was collected and incubated overnight at 25 °C. The samples were discarded if not used on the following day. Lipid phosphorus was determined by a modification of the method of Bartlett (1959), and the cholesterol content was determined by a cholesterol oxidase assay (Allain et al., 1974).

Concentrated stock solutions of BS were prepared by dissolving each BS in a buffer containing 0.15 M NaCl and 5 mM HEPES. The critical micelle concentration (CMC) of each BS in buffer was obtained by surface tension measurements using a digital tensiometer (Model K10T, Krüss). In order to minimize any high local BS concentrations in the solution during sample mixing, all experiments were performed by adding the stock sonicated vesicle dispersion to various diluted BS solutions. In the case of TDC, only lecithin vesicles with 33 mol % CH were examined. In each run, the final lecithin concentration was 1.0 mM, and the final sample volume was set to 2.5 mL. All experiments were performed at room temperature.

Vesicle leakage was determined by a probe encapsulation assay using ANTS and DPX as the fluorescence probes (Ellens et al., 1985). Small unilamellar vesicles were prepared in a buffer containing 12.5 mM ANTS, 45 mM DPX, 60 mM NaCl, and 5 mM HEPES. The vesicles were separated from unencapsulated material by gel filtration on a Sephadex G-75 column, using 0.15 M NaCl and 5 mM HEPES as the elution buffer. All of the above buffer solutions were adjusted to pH 7.0, and were checked to be isosmotic (Osmotte A, Precision Instruments). To inhibit bacteria growth, 0.02 wt % of NaN_3 was added to each buffer. Fluorescence measurements were performed with a Perkin-Elmer MPF-66 spectrofluorometer using an excitation wavelength of 355 nm. Emission was measured continuously at 530 nm, and a 430 nm filter was used to eliminate scattered light. Because of the small initial turbidity and the small changes in sample turbidity observed, inner filter effects are negligible and do not increase with time. The leakage of encapsulated ANTS and DPX from vesicles results in an intensity increase due to the dequenching of ANTS fluorescence. The 0% leakage level was given by the fluorescence intensity of vesicles coencapsulating both probes at the final lecithin concentration. The 100% leakage level was obtained by lysing the vesicles with 3 mM Triton X-100.

In the lipid-mixing assay (Struck et al., 1981), vesicles with 0.6 mol % of each NBD-PE and Rh-PE were prepared with the elution buffer. These labeled vesicles were mixed with vesicles devoid of fluorescent lipids (unlabeled vesicles) at a ratio of 1:4. Excitation was set at 465 nm, and emission was measured continuously at 590 nm with a 570 nm cutoff filter at the emission chamber to eliminate scattered light. Due to the dilution of fluorescence lipids into unlabeled vesicles, the efficiency of energy transfer between NBD-PE (donor) and Rh-PE (acceptor) is lowered, resulting in a decrease in Rh-PE fluorescence at 590 nm. The 0% mixing level (i_o) was given by the fluorescence intensity of the initial vesicle dispersion, and the 100% mixing level (i_∞) was taken as the residual intensity after lysing the vesicles with 3 mM Triton X-100. The 100% level thus indicates complete solubilization of the vesicles into micelles. In an experiment with a labeled-to-unlabeled vesicle ratio of 1:4, either complete vesicle aggregation or complete probe mixing will lead a 5-fold dilution of the fluorescence lipid probes, and so corresponds to a 80% mixing level. A mixing level higher than 80% therefore indicates the formation of mixed micelles.

Vesicle growth was followed by measuring the turbidity at 350 nm with a Perkin-Elmer Lambda 2 spectrophotometer. Vesicles were prepared with the elution buffer, and a blank buffer was used as a reference. In order to examine the increase in vesicle size with time, vesicle growth was also monitored by quasi-elastic light scattering using a BI9000 spectrometer (Brookhaven Instruments Corp.) at a scattering angle of 90°. Samples were placed in a decalin index-matching bath and illuminated with 488 nm light (Lexal 2W Ar^+ laser). All solutions were filtered through 0.2 μm Millipore Acrodisc-13 filters before sample mixing; such filtering did not alter the lipid concentration. The mean diffusion coefficient and the polydispersity index were obtained from the fitted first and second cumulants, using a cumulant analysis of the intensity autocorrelation function of the scattered light, respectively (Koppel, 1972). The mean hydrodynamic radius was then calculated from the Stokes−Einstein relationship (Berne & Pecora, 1976). Since acquisition of the autocorrelation function requires about 1 min, each data point represents an average size of the changing aggregates during that time period. The final particle sizes and polydispersity indexes of all samples were again measured after a 24 h equilibration. The use of dilute lipid solutions in this study ensures that both interparticle interactions and multiple scattering are negligible.

RESULTS

The vesicle-to-micelle transition induced by BS addition can be conveniently followed by turbidity measurements, and Figure 3, for TUDC, shows a typical pattern. At low surfactant-to-lecithin ratios (stage I), monomeric surfactants partition into the lipid bilayers without altering the sizes of vesicles. Upon further increase in surfactant concentration, turbidity increases as vesicles begin to grow. Within this growth regime, the values of turbidity after equilibration

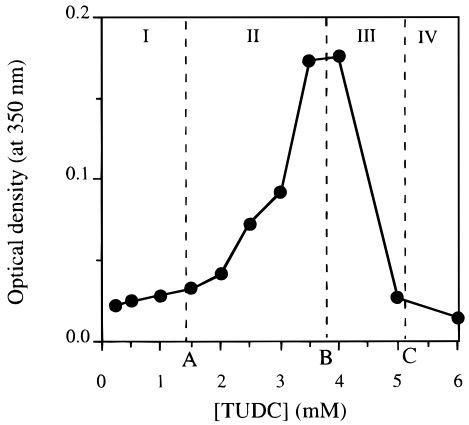

FIGURE 3: Turbidity changes associated with the vesicle-to-micelle transition. Sonicated *pure* lecithin SUV were added to different TUDC concentrations, and the turbidity at 350 nm was measured after equilibration for 24 h. Final lecithin concentration was 1 mM, and the final sample volumes were held constant at 2.5 mL. Stage I, partitioning of bile salts between the vesicle bilayer and the aqueous phase; stage II, vesicle growth; stage III, coexistence of large vesicles and mixed micelles; stage IV, complete solubilization of vesicles into BS−L mixed micelles.

either increase (stage II) or decrease (stage III) with surfactant concentration. Finally at high surfactant-to-lecithin ratios, turbidity decreases drastically, and vesicles are completely solubilized into small stable mixed micelles (stage IV). These observations confirm and extend those of Lichtenberg et al. (1990) with taurocholate as the bile salt. In addition, we have systematically examined here the effects of both bile salt hydrophobicity and cholesterol content on the growth of CH−L vesicles.

Bile Salt−Vesicle Interaction: Stage I. For concentrations of up to 1 mM of either TC (Figures 4a,b, 5a,b) or TUDC (Figures 4d,e, 5d,e), both turbidity and vesicle size remain unchanged for at least 1 h after the vesicles are exposed to BS. When vesicles contain 33 mol % CH, there are no changes in turbidity and vesicle sizes at concentrations of up to 2 mM of either TC or TUDC (Figures 4c, 4f, 5c, 5f). Thus, high levels of CH apparently stabilize lecithin vesicles. Despite the reluctance of vesicles to undergo size change, low concentrations (<1 mM) of either TC or TUDC induce considerable leakage and promote intervesicular lipid mixing for pure lecithin vesicles (Figures 6a, 7a, 6d, 7d). Leakage occurs gradually with time under these conditions, and the leakage rates correlate with BS concentrations. In the absence of cholesterol, TUDC is more efficient than TC in causing vesicle leakage (Figures 6, 8). Leakage of vesicles containing 20 mol % CH is still substantial, but the effects of TC and TUDC are comparable (Figures 6, 8). In sharp contrast, with less than 2 mM TC or TUDC, vesicles containing 33 mol % CH do not leak over a period of 1 h. Although high levels of CH retard vesicle leakage, the overall rates of lipid mixing are insensitive to CH content (Figure 9). In all cases, the onset of lipid mixing occurs at a lower BS concentration than does vesicle leakage, with this phenomenon especially obvious with CH-rich vesicles (Figures 6 and 7).

Bile Salt−Vesicle Interaction: Stage II. In this regime, the concentrations of both TC and TUDC lie around 1−3 mM and 2−4 mM for vesicles containing respectively below 20 mol % CH and with 33 mol % CH. At these concentrations, both solution turbidity and vesicle size increase with

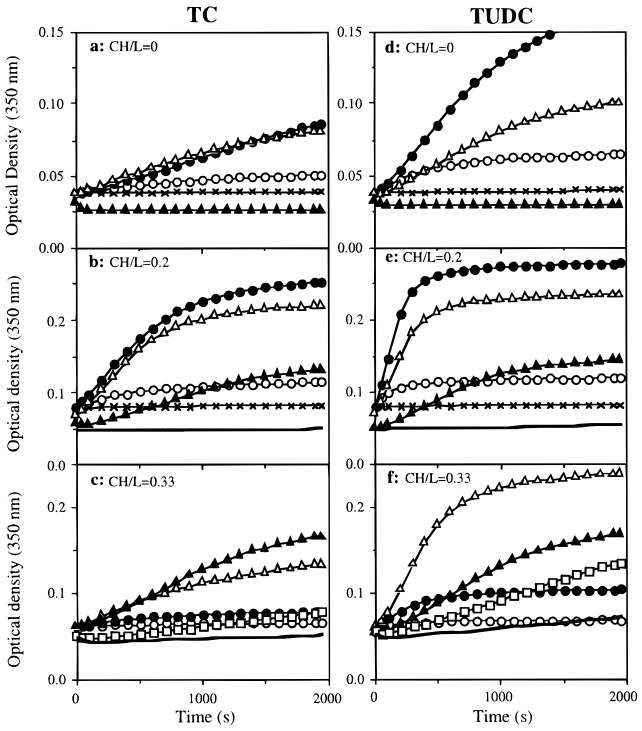

FIGURE 4: Bile salt-mediated vesicle growth as monitored by the optical density (turbidity) at 350 nm as a function of time. Panels a−c and d−f show respectively the effects of TC and TUDC on vesicle stability. A buffer solution containing no vesicles was used as reference. At time zero, lecithin vesicles containing (a, d) 0 mol % CH, (b, e) 20 mol % CH, and (c, f) 33 mol % CH were added to a bile salt solution. A number of TC and TUDC concentrations (in mM) were used: (×) 1; (○) 2; (●) 3; (△) 4; (▲) 5; (□) 6; (—) 8. Final lecithin concentration used was 1 mM, and the sample volumes were held constant at 2.5 mL.

time after sample mixing (Figures 4 and 5). The rates of these increases scale with BS concentrations. The final values of turbidity and vesicle size (after 24 h equilibration) show that TUDC consistently produces slightly larger vesicles than TC. The polydispersity indexes of all final samples are low, suggesting that a negligible number of micelles are formed under these conditions (Figure 10).

For CH contents below 20 mol %, vesicle leakage and lipid mixing take place almost instantaneously after sample mixing. Since massive leakage occurs under these conditions, the observed vesicle growth does not follow the typical mechanistic pathway describing "non-leaky" vesicle fusion. On the other hand, despite rapid lipid mixing, leakage of vesicles containing 33 mol % CH is negligible (Figure 6). In this regime, cholesterol also slightly reduces the extent of lipid mixing (Figure 7). Despite the absence of any noticeable initial decrease in turbidity, the sudden jump in the initial lipid mixing data must be due to a small extent of micellization (Figure 7). This transient micelle formation could be a consequence of locally large BS/L due to nonhomogeneous sample mixing.

Bile Salt−Vesicle Interaction: Stage III. With higher BS concentrations, the increase in turbidity with time follows a different profile. Immediately following sample mixing, turbidity drops and then rises gradually after a short time lag (Figure 4). The magnitude of the turbidity drop increases with BS concentration, and this initial decrease can be attributed to instantaneous micelle formation. A similar profile for BS-induced vesicle growth has been observed by

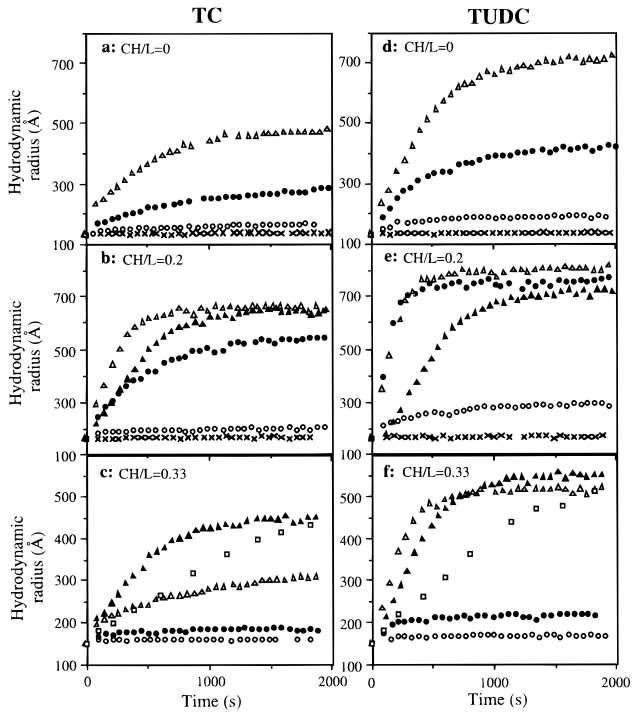

FIGURE 5: Bile salt-mediated vesicle growth as monitored by QELS as a function of time. At time zero, lecithin vesicles containing (a, d) 0 mol % CH, (b, e) 20 mol % CH, and (c, f) 33 mol % CH were added to a bile salt solution. Panels a-c and d-f show respectively the effects of TC and TUDC on vesicle growth. All solutions were prefiltered, and the scattering angle was set at 90°. The mean particle diffusion coefficient was obtained from the fitted first cumulant using a cumulant analysis of the intensity autocorrelation function of the scattered light, and the mean hydrodynamic radius was calculated using the Stokes−Einstein relationship. Each data point represents an average size of the growing particles during the time period required for acquiring the autocorrelation function (∼1 min). Both experimental conditions and symbols for TC or TUDC concentrations are as described in Figure 4.

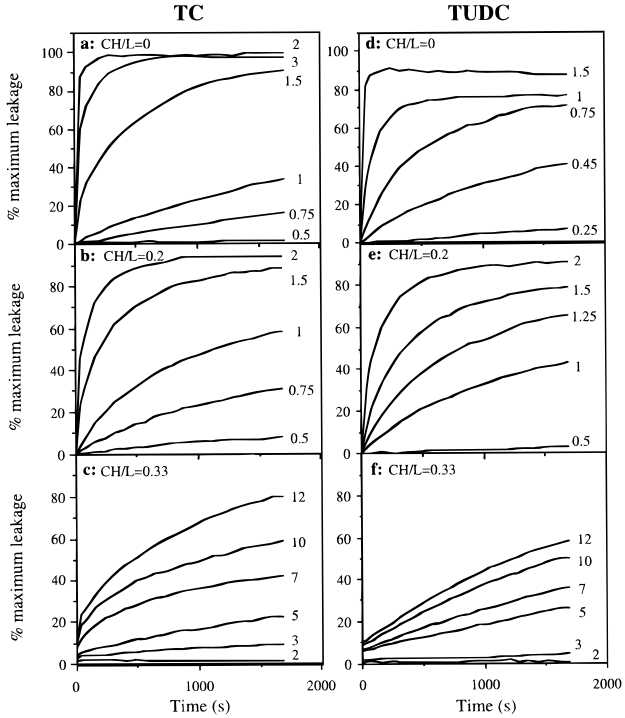

FIGURE 6: Bile salt-induced vesicle leakage of internal contents as probed by the ANTS/DPX fluorescence encapsulation assay as a function of time. Bile salt concentrations are shown by their corresponding leakage curves. Panels a-c and d-f demonstrate the effects of TC and TUDC on vesicle leakage, respectively. Excitation and emission wavelengths were set at 355 and 515 nm, respectively, and a 430 nm filter was used to eliminate scattered light. Experimental conditions are as described in Figure 4.

Lichtenberg et al. (1990) at high total lipid concentration. The final turbidity values decrease with increasing BS concentrations (Figure 4) and are always lower than the maximum value registered in stage II, thus contributing to the bell-shaped turbidity−concentration curve indicative of vesicle-to-micelle transitions (Figure 3). On the other hand, QELS size measurements of samples with identical BS concentrations show neither an initial decrease in size nor an associated lag time (Figure 5). Since the time necessary for acquiring the autocorrelation functions is about 1 min, the sizes reported after mixing only reflect the average size of the particle within that data acquisition period. Furthermore, because the *z*-average intensity weighting intrinsic to the cumulant analysis is biased toward larger particles, no initial decrease in particle size is evident unless a substantial number of small mixed micelles have formed. If wormlike micelles form under these conditions, there will not be a large decrease in the measured particle size (Egelhaaf & Schurtenberger, 1994).

In the case of pure lecithin vesicles, the peak of the turbidity−concentration curve signifies the onset of the vesicle−micelle coexistence region (Edwards & Almgren, 1992). After exposure to 4 mM TC or TUDC, equilibrated samples that are prepared using pure lecithin vesicles are indeed highly polydisperse (Figure 10). Double exponential analysis of the autocorrelation functions collected from these samples reveals two particle populations with sizes characteristic of large vesicles ($\bar{R}_h$ ∼350 Å) and mixed micelles ($\bar{R}_h$ ∼100 Å). Vesicles containing 20 mol % CH become highly polydisperse (PI > 0.1) only above 5 mM TC or TUDC. Similarly, samples containing 33 mol % CH have low PI even at concentrations up to 6 mM TC or TUDC. In other words, CH pushes the onset of the micelle−vesicle coexistence region toward higher BS concentrations and expands the micellar shoulder of the transition curve (Figures 11c and 12). These mixtures remain stable over time, and no macroscopic phase separation is observed after a week of equilibration.

For vesicles containing less than 20 mol % CH, both leakage and lipid mixing occur instantaneously after the sample is mixed (Figures 6 and 7). Leakage is moderately repressed up to 5 mM TC or TUDC for vesicles containing 33 mol % CH. This inhibiting effect of CH is more pronounced for TUDC than for TC (Figure 8). Extensive leakage occurs only at TC or TUDC concentrations higher than 10 mM, suggesting again that excess BS is required to achieve complete micellization of CH-rich vesicles.

Bile Salt−Vesicle Interaction: Stage IV. Upon the addition of 5 mM TC or TUDC, pure lecithin vesicles are completely solubilized into mixed micelles, as depicted by the instantaneous decrease in turbidity (Figure 4a,d) and vesicle size (Figure 10). Unlike stage III, the turbidity drops remain low and steady. The final polydispersity indexes of these samples are low, and the average final hydrodynamic radii of TC−L−CH mixed micelles and TUDC−L−CH mixed micelles are 100 Å and 68 Å, respectively. Because the primary focus of this work is elucidation of the mechanism of vesicle growth in stage II, our experimental protocol was not extended to explore the already well-

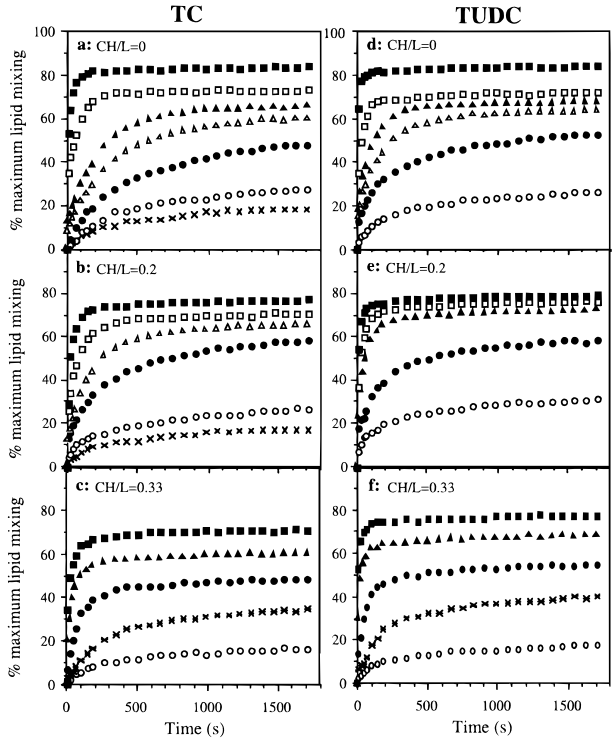

FIGURE 7: Bile salt-induced mixing of membrane lipids as a function of time. Labeled vesicles with 0.6 mol % each of NBD-PE and Rh-PE were mixed with unlabeled vesicles at a molar ratio of 1:4. Panels a-c and d-f show the effects of TC and TUDC on the extent of lipid mixing, respectively. Due to the exchange of NBD-PE into unlabeled vesicles, the efficiency of resonance energy transfer from NBD-PE (donor) to Rh-PE (acceptor) is reduced, resulting in a decrease in Rh-PE fluorescence at 590 nm. Excitation and emission wavelengths were set at 465 and 590 nm, respectively, and a 570 nm cutoff filter was used to eliminate scattered light. A number of TC or TUDC concentrations (in mM) were used: (×) 0.25; (○) 0.5; (∗) 0.75; (●) 1; (△) 1.5; (▲) 2; (□) 3; (■) 4. Experimental conditions are as described in Figure 4.

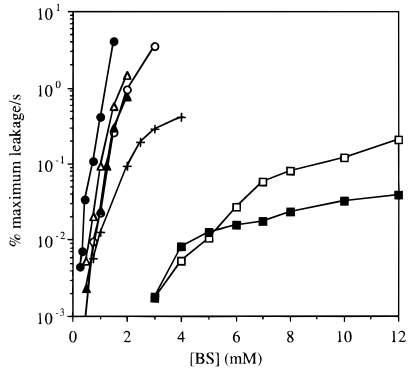

FIGURE 8: Rate of vesicle leakage as a function of bile salt concentrations. The leakage rates in terms of percentage maximum leakage per second are calculated from the initial slopes of the leakage curves as depicted in Figure 6. Circles, triangles, and squares represent the leakage rates for lecithin vesicles containing 0, 20, and 33 mol % CH, respectively. Open symbols denote samples with TC and filled symbols those with TUDC. Crosses (×) denote the rates of TDC-induced leakage of vesicles containing 33 mol % CH.

characterized state of complete micellization, especially for CH-containing vesicles that require a large BS/L (Lichtenberg et al., 1990).

Vesicles containing 33 mol % CH show similar structural changes in the presence of the hydrophobic bile salt TDC (Figure 12). Vesicles begin to grow after exposure to only

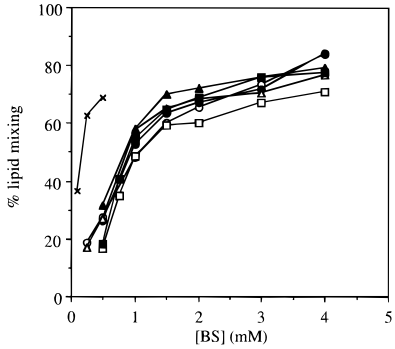

FIGURE 9: Extent of lipid mixing as a function of bile salt concentrations. Data points are taken from Figure 7 30 min after sample mixing. Symbols employed are identical to those in Figure 8.

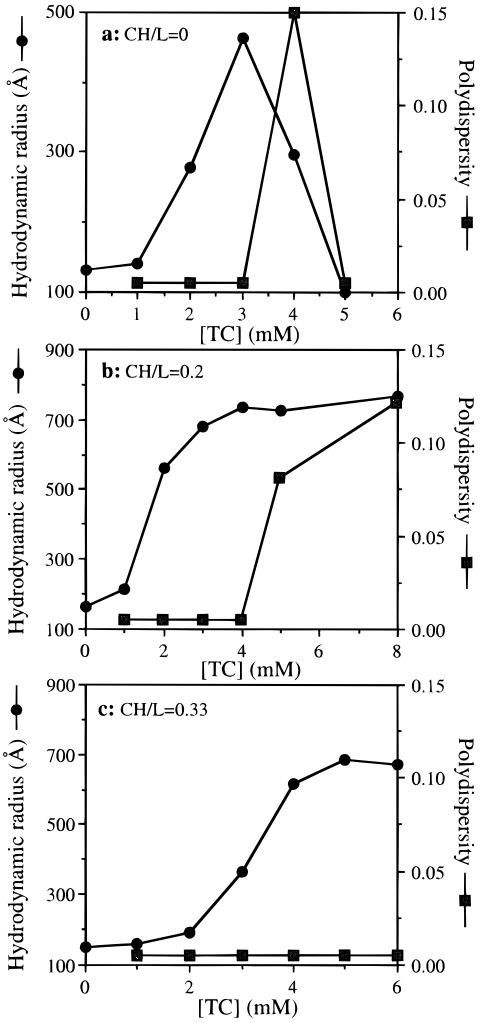

FIGURE 10: Quasi-elastic light scattering on equilibrated samples. Hydrodynamic radii (●) and polydispersity indexes (■) measured after 24 h are plotted as a function of TC concentrations, with vesicles containing (a) 0, (b) 20, and (c) 33 mol % CH. Hydrodynamic radii were calculated as described in Figure 5. Polydispersity indexes are calculated from the second cumulant. Results for TUDC are similar to those for TC.

0.2 mM TDC (Figure 12). Our surface tension measurements showed that the critical micelle concentrations (CMC) of TC, TUDC, and TDC are 4.5 mM, 2.2 mM, and 1.2 mM, respectively. As expected, the more hydrophobic TDC partitions into the bilayers more readily than does either TC or TUDC (Bayerl et al., 1989). Thus, TDC induces the aforementioned structural changes of vesicles at lower

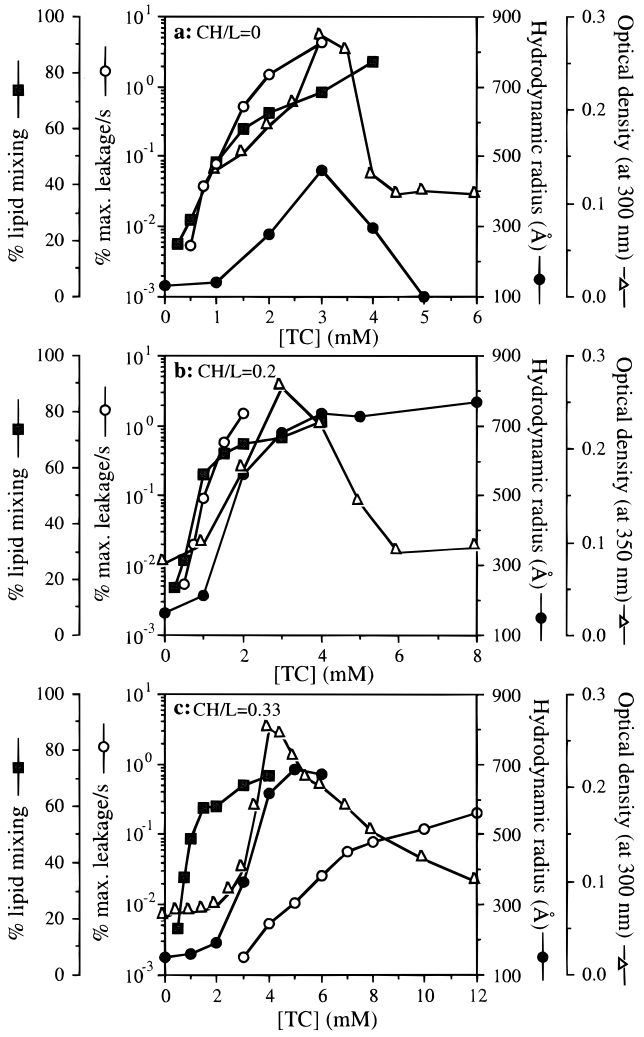

FIGURE 11: Overall progression of TC-induced structural changes of vesicles. Changes of lecithin vesicles containing (a) 0, (b) 20, and (c) 33 mol % CH were plotted versus TC concentrations. Optical densities of samples (△) were measured 24 h after sample mixing. Hydrodynamic radii (●) are obtained as described in Figure 5. The rates of vesicle leakage (○) and the extent of lipid mixing (■) are obtained as described in Figures 8 and 9, respectively. Results for TUDC are similar to those of TC.

concentrations than does either TC or TUDC. Cholesterol likewise inhibits TDC-induced vesicle leakage and expands the micellar side of the turbidity−concentration transition curve.

In summary, complete leakage and rapid lipid mixing precede both TC- and TUDC-induced growth and solubilization of pure lecithin vesicles (Figure 11a). Pure lecithin vesicles are completely solubilized after exposure to 5 mM of either TC or TUDC (Figure 11a). Vesicles containing 20 mol % CH behave in a similar fashion (Figure 11b), except that complete micellization is not achieved even upon exposure to 8 mM TC or TUDC (reflected by the high PI at 8 mM TC and TUDC as depicted in Figure 10b). When 33 mol % CH is present in vesicles, leakage is significantly reduced, and the vesicle-to-micelle transition is further broadened to higher BS concentrations (Figure 11c). Finally, the more hydrophobic TDC solubilizes vesicles at lower concentrations than are effective for TC and TUDC (Figures 11c and 12). At a constant lipid concentration (1 mM in this study), the structural changes associated with CH−L vesicles, as well as the ultimate states of lipid aggregates in bile, therefore depend strongly on the CH content of the vesicles and the hydrophilic−hydrophobic balance of the BS mixture.

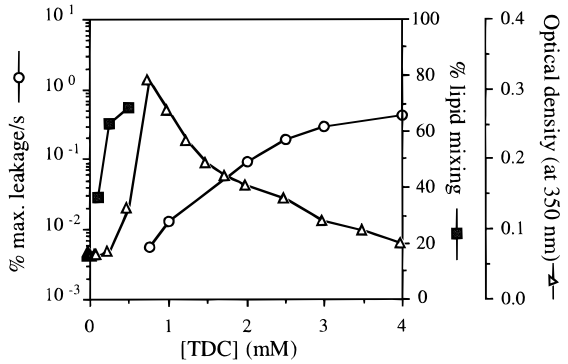

FIGURE 12: Overall progression of TDC-induced structural changes of vesicles containing 33 mol % CH. Symbols employed are identical to those of Figure 11. Note that the vesicle-to-micelle transition takes place at a much lower concentration of TDC than of TC or TUDC.

DISCUSSION

The initial stage of bile equilibration *in vivo* primarily involves the interactions between freshly secreted CH−L vesicles and free bile salts. The secreted vesicles are partially solubilized to form mixed micelles, and this process leads to the formation of highly metastable CH-rich vesicles (Cohen et al., 1990). According to the equilibrium BS−L−H_2O phase diagram, the transition from lamellar vesicles to micelles transverses two coexistence regions that contain the hexagonal phase, which consists of hexagonally-packed infinitely long cylinders[2] (Small et al., 1966). At the lecithin concentration used in this study (1 mM or ∼0.08 wt %), those transitions occur at approximately 3.5 mM and 3.8 mM TC, respectively (Figure 1). These TC concentrations correspond closely to the breakpoints at the vesicle−micelle coexistence region of the turbidity curve (stage III) obtained for pure lecithin vesicles (Figure 10a). By holding the total volume constant, the experimental course of the BS-induced vesicle solubilization explored in this study follows a path that is the reverse of BS removal by dialysis (Figure 1).

In order to generalize the observed vesicle-to-micelle transition, Lichtenberg et al. (1983) have suggested use of an "effective" bile salt-to-lecithin ratio, R_e

$$R_e = \frac{[BS]_{total} - [BS]_{aqueous}}{[L]} \quad (1)$$

or

$$[BS]_{total} = [BS]_{aqueous} + R_e[L] \quad (2)$$

where [L] is the lecithin concentration. R_e thus represents the BS/L of the *single* existing lipid aggregate. The concentration of monomeric lecithin is assumed negligible. The aqueous BS concentrations, $[BS]_{aqueous}$, that are in equilibrium with either micelles or vesicles are respectively called the intermicellar concentration (IMC) or the interve-

[2] The hexagonal phase has not yet been observed in dilute bile. On the basis of small-angle neutron scattering spectra, the indicated hexagonal phase regions in the dilute regime of Figure 1 are believed to contain only long rodlike BS−L mixed micelles of finite length.

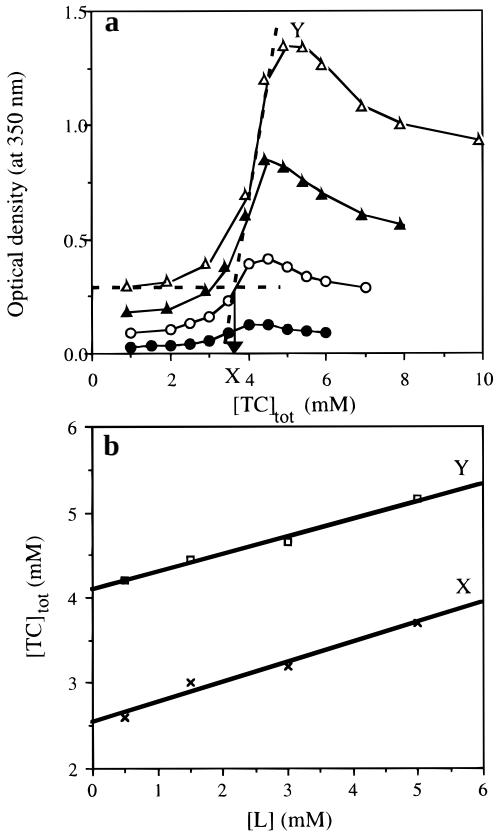

FIGURE 13: Experimental determination of R_e and $[BS]_{aqueous}$ from turbidity measurements. (a) Series of turbidity plots, characteristic of vesicle-to-micelle transitions, are shown as a function of lecithin concentrations. Turbidity values were obtained 24 h after BS addition to lecithin vesicles containing 33 mol % CH. Lecithin concentrations (in mM) employed were (●) 0.5, (○) 1.5, (▲) 3,; and (△) 5. Two of the key transitions are identified from the plots. Point A was obtained from the intersection of the two tangents constructed from the vesicular shoulder of the turbidity plots. Point B was given by the maximum of the turbidity curves. (b) The compositions of BS and L corresponding to point A (×) and point B (□) lie on a straight line. The slope of the line represents the effective BS/L of the existing aggregates, R_e, at that specific transition point, and the *y*-intercept gives the aqueous BS concentration, $[BS]_{aqueous}$, that is in equilibrium with those aggregates, often referred to as the IMC or the IVC. As indicated, this estimate of $[BS]_{aqueous}$ depends on the choice of the reference transition point.

sicular concentration (IVC). Both concentrations are lower than the CMC of the pure component BS (Donovan et al., 1993). These concentrations can be measured directly by either equilibrium dialysis or ultrafiltration (Donovan et al., 1993). Otherwise, both R_e and $[BS]_{aqueous}$ must be indirectly calculated from experiments.

Turbidity records are commonly used to trace either the process of vesicle solubilization or the reverse process of dilution of concentrated mixed micellar solutions (Figure 3). With increasing total BS concentration, the bile salt content of vesicles, or R_e, goes up. Since the amount of BS required for solubilization increases with the number of lecithin vesicles, the solubilization curve shifts toward higher bile salt concentration with increasing lecithin concentration (Figure 13a). As described by Schurtenberger et al. (1985), a set of concentration data can be extracted from similar points along each of the solubilization curves (the onset of turbidity increase X and the local maximum Y in Figure 13a), and those bile salt and lecithin concentrations fall on a straight line (Figure 13b). According to eq 2, the slope and the *y*-intercept of the resultant straight line yield R_e and $[BS]_{aqueous}$, respectively, at that *particular* point in the solubilization process.[3]. Depending on which lipid aggregate is present (micelle or vesicle), the $[BS]_{aqueous}$ is defined accordingly as the IMC or the IVC. Given a BS with a known IMC or IVC, the changes observed at a certain R_e value can therefore be extended to predict similar changes at higher (physiological) lecithin concentrations such as those found in human bile. In order to establish the relationship between the fate of fresh biliary vesicles and the onset of CH gallstone formation, the molecular events involved in the structural changes of CH-rich vesicles must be carefully examined.

Intervesicular Exchange or Mixing of Lipids. In the absence of vesicle growth or disruption, lipids exchange spontaneously between vesicles via aqueous diffusion (McLean & Phillips, 1981). At lecithin concentrations of about 10 mM, significant amounts of lipids also exchange during vesicle collisions (Jones & Thompson, 1989). The physiological lecithin concentrations in human bile (∼20−60 mM) are at levels adequate for lipid transfer to proceed through both mechanisms. Low levels of bile salts further promote intervesicular lipid exchange without vesicle solubilization, probably by increasing the aqueous solubility of lipid monomers and accelerating the absorption and desorption of lipids from vesicles (Nichols, 1986). Our experiments likewise show that BS enhances intervesicular lipid mixing at a concentration well before vesicles start to either leak or grow. In the case of vesicles containing 33 mol % CH, lipid mixing is almost complete at 2 mM TC or TUDC, and there is no detectable leakage (Figures 6c,f, 7c,f). In addition, at a fixed BS/L, the degree of lipid mixing increases as BS becomes more hydrophobic (Nichols, 1986). Our results similarly show that the most hydrophobic TDC induces intervesicular lipid transfer at lower concentrations than does TC or TUDC (Figures 11 and 12).

Vesicle Leakage. Leakage of pure lecithin vesicles occurs well before either vesicle growth or micellization (Figures 5 and 6). Because there is no lag time between sample mixing and the onset of leakage (Figure 6), the binding of BS to vesicles must be fast. Immediately after BS addition, BS binds to the outer monolayer of the vesicles and disorganizes the lipid hydrocarbon chains (Ulmius et al., 1982; Schubert et al., 1986). All of the bound bile salts initially accumulate in the outer leaflets of the lipid membranes. Because of the extremely slow flip-flop rates of lecithin and taurine-conjugated BS (Kamp & Hamilton, 1993), the asymmetric membrane distribution of these BS may impose additional bending stresses on the already highly curved bilayers of SUV. In order to relieve the growing bending stresses, vesicles probably open up, at least momentarily, for BS to equilibrate between the inner and outer monolayers. In similar studies with other surfactants, cryo-TEM images are able to capture these possibly porous or open vesicles (Walter et al., 1990). This type of vesicle leakage is believed to proceed via the formation of transient pores, probably as BS reverse micelles, within the membranes (Schubert & Schmidt, 1988). The gradual

[3] According to Lichtenberg (1985), the point of complete solubilization of vesicles occurs when the BS/L of the vesicles reaches a constant critical value, $\bar{R}_e^c$.

noninstantaneous leakage that is observed at low BS/L further supports the transient nature of these pores (Figure 6).

The onset of vesicle leakage also depends on BS hydrophobicity and the CH content of the vesicles. During membrane opening, hydrophobic BS is more effective than hydrophilic BS in shielding the exposed lipid hydrocarbon tails. At the same lecithin concentration, TDC (CMC ~1.2 mM) is more effective than TC (CMC ~4.5 mM) in causing leakage of vesicles containing 33 mol % CH (Figures 11c and 12). On the other hand, the presence of CH in vesicles retards BS-induced leakage (O'Connor et al., 1985; Schubert & Schmidt, 1988). With 20 mol % CH in the membrane, leakage is slightly reduced, and this stabilizing effect might result from rapid transbilayer movement of CH (Lange et al., 1977). Cholesterol movement to the inner bilayer can dissipate the increase in membrane stresses induced by BS addition, so CH-rich vesicles can accommodate more BS than do CH-poor vesicles before leakage ensues. In the presence of 33 mol % CH, leakage is drastically attenuated (Figure 6). For concentrations above ca. 30 mol % CH, the onset of lipid phase segregation (i.e., the formation of CH- and L-rich microdomains within the membrane) could play a role in the apparent strengthening of the bilayers (Yeagle, 1985).

Vesicle Growth. Bile salts, even at concentrations below their CMC, can stimulate the growth of SUV in dilute solution (Alonso et al., 1982). On the basis of turbidity and QELS measurements, growth of lecithin vesicles begins at about 2 mM of either TC or TUDC (Figures 4 and 5). For BS concentrations that correspond to stage II of the transition, the measured turbidity increases continually within the experimental time scale and without an observable lag time (Figure 4). Substantial vesicle leakage at these BS concentrations makes all fusion assays based on probe encapsulation ineffective. Because such concentrations of BS also promote considerable intervesicular lipid exchange (Figure 7), fusion assays based on the mixing of lipid probes (Struck et al., 1981) also can no longer unambiguously identify vesicle fusion. Although we cannot experimentally examine the possible ongoing of vesicle fusion, the results reported here do provide valuable information about the structural mechanisms of BS-induced vesicle growth.

Two plausible mechanisms have been proposed for general surfactant-induced vesicle growth. In the first mechanism, the bilayers rapidly reseal or reclose after leakage (Schubert et al., 1991). The subsequent vesicles can then grow by typical aggregation and fusion pathways (Bentz & Ellens, 1988; Edward & Almgren, 1992). Since all taurine-conjugated bile salts are anionic (pK_a ~2) at pH 7, BS−L mixed vesicles are negatively charged, and there is a net electrostatic repulsive force between vesicles. With increasing amounts of bound BS, the magnitude of this repulsion strengthens, and the vesicles are less likely to undergo colloidal aggregation. On the contrary, the rate of the observed vesicle growth increases with BS concentration within stage II of the solubilization curve (Figures 4 and 5). Moreover, previous gel filtration chromatography studies from our group demonstrate that BS addition to vesicles causes a noticeable increase in the CH/L of vesicles (Little et al., 1991). Obviously, a net transfer of both CH and L to the growing vesicles must be taking place, but no change in CH content should occur if vesicle aggregation and fusion are the primary growth mechanism.

In the second mechanism, vesicles grow by diffusion of lipid molecules through the aqueous medium (Papahadjopoulos et al., 1976; Almog et al., 1986). This mechanism also describes vesicle aging, a slow relaxation process where small metastable vesicles minimize the large bending energy associated with their highly curved bilayers by reverting to large vesicles (Madani & Kaler, 1990). Large unilamellar vesicles, having a low bending energy, therefore do not grow in the presence of surfactants (Alonzo et al., 1982). In analogy to the process of vesicle aging, vesicles grow by aqueous diffusion as BS increases the transfer fluxes of lipids between vesicles (Nichols, 1986). Hence, the rate of vesicle growth increases with BS concentration (stage II). Furthermore, in support of this hypothesis, the spontaneous intervesicular transfer rate of CH between vesicles is much faster than the transfer rate of lecithin (McLean & Phillips, 1981). Since BS raises the aqueous CH solubility, the intervesicular transfer rates of CH will also be amplified (Bruckdorfer & Sherry, 1984). This difference in the transfer fluxes of CH and L may explain the formation of large CH-enriched vesicles in gallbladder bile (Little et al., 1991; Cohen et al., 1992).

A different growth profile predominates at slightly higher BS/L (stage III). In this stage, the turbidity initially drops and gradually increases with time. This phenomenon is especially obvious for vesicles containing CH (Figure 4). Because BS concentrations in this regime are close to or higher than the intermicellar concentration (IMC), the initial turbidity drop probably signifies partial solubilization of vesicles. With increasing amount of added BS, the initial drop in turbidity becomes more pronounced as more of the smaller micelles are initially formed (Figure 4). On the basis of QELS measurements, these samples after 24 h equilibration are highly polydisperse, and the final measured sizes of the lipid aggregates demonstrate the coexistence of vesicles and micelles (Figure 10). Dilution of TC−L, TDC−L, or TUDC−L mixed micellar solutions similarly yields micelle−vesicle coexistence regions at this stage of the transition (Long et al., 1994b; Liu et al., 1994). Vesicle growth observed at this stage resembles the profile corresponding to the growth of vesicles following the dilution of a concentrated cholate−lecithin mixed micellar solution (Almog & Lichtenberg, 1988). Lichtenberg et al. (1990) suggest that the sigmoidal growth profile reflects the spontaneous partial revesiculation of the metastable CH-supersaturated mixed micelles formed upon solubilization, followed by growth of the "reassembled" vesicles. An earlier study by our group (Little et al., 1991), in which vesicles and micelles were separated by gel chromatography after the exposure of CH−L vesicles to bile salts, showed that both the size and the cholesterol content of the remaining vesicles are larger than those of the parent vesicles. If only micellar recombination was responsible for vesicle growth, the overall CH/L of the final large vesicles should fall, considering that the BS−L−CH mixed micelles are less effective in solubilizing CH than are the parent vesicles. Therefore, the "reassembled" vesicles must also grow by the aqueous transfer of CH and L as described previously.

Four different techniques have been used to probe carefully the integrity of CH−L vesicles after exposure to submicellar concentrations of BS. Commonly used turbidity measurements are not sensitive to all of the important morphological changes, and so can be used only to establish the bounds

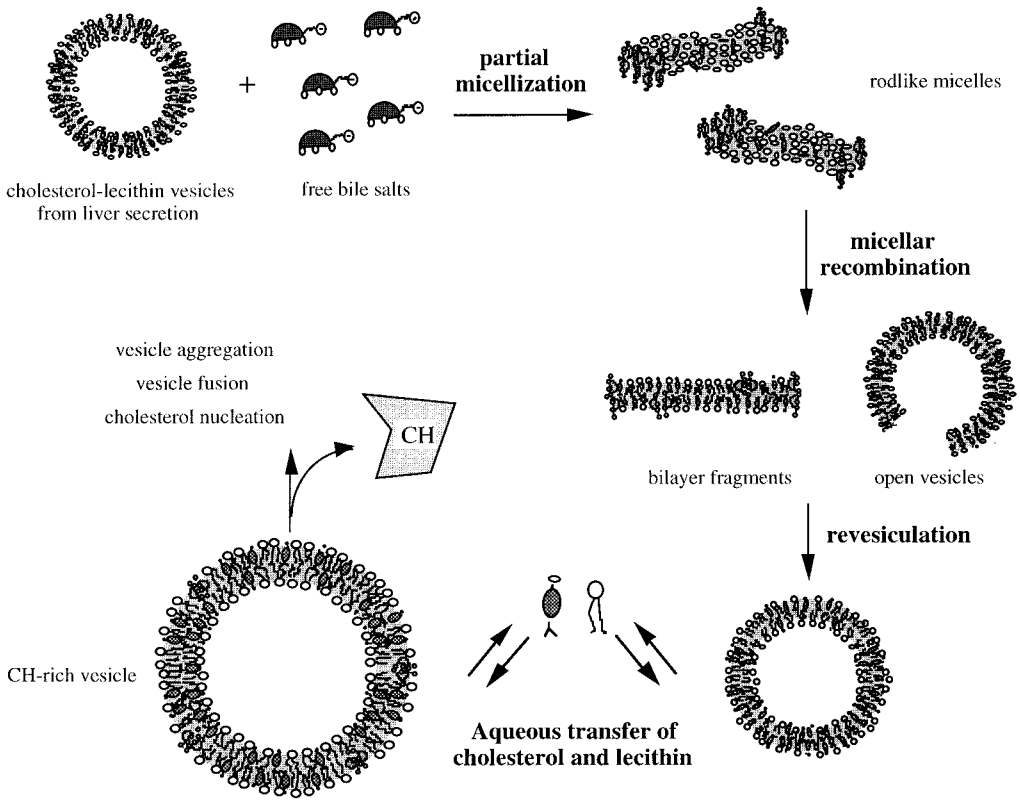

FIGURE 14: Hypothesized diagrammatic representation of bile equilibration and cholesterol gallstone formation. The freshly secreted cholesterol−lecithin vesicles from liver are partially solubilized to mixed micelles by bile salts, which are independently secreted. The supersaturated mixed micelles partially recombine into vesicles through a number of intermediates such as bilayer fragments or open vesicles. The degree of recombination depends on the CH/L and the BS/L of the solutions. Some of these vesicles will again be solubilized when subjected to the concentrating effect in the gallbladder. During the whole equilibrating process, vesicles grow by lipid transfer via either aqueous diffusion or collision. The resultant highly metastable cholesterol-rich vesicles are prone to aggregate and fuse, and thus become the precursors to cholesterol gallstones.

of the overall vesicle-to-micelle transition. To determine whether the observed increase in turbidity corresponds to vesicle growth, QELS was used to measure the hydrodynamic radius and polydispersity of the lipid aggregates. For conditions setting stage II of the transition, both turbidity and particle size increase with time. The final equilibrated samples in this regime (after 24 h) are monodisperse, so vesicles grow without significant micelle formation. Quasi-elastic light scattering, however, does not provide information about structural intermediates (such as open vesicles) that could be present, nor does it allow determination of micelle shape. We note that QELS measurements at different scattering angles can allow resolution of particle shapes (Egelhaaf & Schurtenberger, 1994). To augment the information from turbidity and scattering measurements, we turned to two fluorescence assays, which are capable of providing insights into the temporal rearrangements of the vesicles after exposure to submicellar levels of BS. Ultimate buttressing of these results could come from cryo-TEM visualization of final and intermediate structures, such as reported by Walter et al. (1991).

Physiological Implications. The observed structural changes of vesicles induced by BS in dilute solutions also occur at high physiological lipid concentrations. A number of minor differences should, however, be addressed. First, at high lipid concentration, the entire solubilization curve will be shifted to the range of BS concentrations that is above the IMC or the CMC. In other words, BS addition to vesicles will most probably lead to micelle production as well as vesicle growth (Lichtenberg et al., 1990). As described previously, vesicle growth will hence involve both initial micellar recombination and subsequent transfer of CH and L between "reassembled" vesicles (Figure 14). Second, vesicles and micelles may undergo macroscopic separation at high lipid concentrations (Lee & Sekijima, 1991), commonly known as gallbladder stratification (Thureborn, 1966). The hexagonal phase, probably formed by the growth of BS−L rodlike mixed micelles, may also emerge in physiological bile solutions (Cohen et al., 1990). Finally, besides aqueous diffusion alone, significant lipid transfer can also occur during vesicle collisions at high lecithin concentrations (Jones & Thompson, 1989). Both transfer pathways can therefore be of physiological importance in the growth of CH−L vesicles in human bile.

Even though TDC and TUDC are both dihydroxyl bile salts, TDC begins to destabilize vesicles at much lower concentrations (Figures 11 and 12). Given that the CMC of TC is twice that of TUDC, solubilization of CH−L vesicles by TUDC and the hydrophilic TC still occurs at similar concentrations (Figures 4 and 5), and TC micelles have a much higher CH solubility than do TUDC micelles (Armstrong & Carey, 1982). Although TC may have a larger lipid solubilizing effect than does TUDC, there are few comparative studies of the effects of TUDC on lipid vesicles. The lipid solubilizing capacity of a particular bile salt is a property of the equilibrium micelles, and need not be directly related to the disruptive effect the bile salt has on vesicle structure. The apparent hydrophilic behavior displayed by

TUDC is due to the geometrical obstruction of its hydrophobic face by the out-of-plane 7β-hydroxyl group (Figure 2). Because of its unique shape, it is proposed that TUDC occupies the apolar interior in the lipid bilayers, similar to the binding sites of membrane cholesterol (Güldütuna et al., 1993). With increasing amounts of CH, TUDC may thus become less efficient than TC in causing vesicle leakage (Figure 8), and vesicles containing 50 mol % CH show almost no leakage in the presence of TUDC (Heuman & Bajaj, 1994). These unique properties of TUDC may also protect CH-rich membranes from damage by other hydrophobic bile salts (Sagawa et al., 1993), and may even inhibit the overall CH nucleation process by stabilizing CH-rich vesicles (Tazuma et al., 1989). The observed similarity between TC and TUDC does not allow us to make comparisons of their disruptive effects on vesicles.

Cholesterol gallstone formation in bile is a highly dynamic and complex event. Our results provide key mechanistic insights into the physiologically relevant events associated with cholesterol solubilization in human bile. The experiments reported here mimic the structural changes experienced by the secreted CH−L vesicles during the early stages of bile equilibration. Secreted vesicles generally have a CH/L of about 0.3 (ca. 23 mol % CH) (Cohen et al., 1992). The range of CH contents employed here thus provides a good representation of both unsaturated and supersaturated biles. If CH/L of the secreted vesicles is high, the final equilibrated vesicles will be highly supersaturated. We have previously demonstrated that the rates of vesicle aggregation and fusion induced by pro-nucleating proteins increase with the cholesterol content of the vesicles (Luk et al., 1993, 1996). By increasing the CH/L of the remaining large vesicles, BS can thus indirectly shorten the CH crystallization time by producing CH-enriched vesicles that are highly susceptible to protein-induced vesicle growth in the gallbladder (Figure 14). On the other hand, BS may also directly accelerate the lateral phase separation of CH from lecithin bilayers. These effects may explain why bile becomes more metastable with increasing total BS/L (Kibe et al., 1985; Harvey et al., 1987). By the same token, amphiphilic proteins can possibly become "secondary" pro-nucleators by either exercising their surface-active properties (Ahmed et al., 1994) or acting as transfer carriers that facilitate aqueous diffusion of CH and L monomers (Corradini et al., 1991).

Given suitable conditions in the gallbladder, CH-rich vesicles are prone to produce CH crystals. This study reinforces the notion that factors which alter the phase behavior of human bile, such as BS hydrophobicity and lipid concentration, play an important and fundamental role in the destabilization of biliary vesicles and thus in the onset of cholesterol gallstone formation. By the same token, bile salts in submicellar concentrations can have important interactions with the lipid bilayers of cells and cellular organelles, leading to dramatic alterations in cell biologic function (Klinkspoor et al., 1995). The results of this study can also provide insights into the cytotoxicity of bile salts.

REFERENCES

Admirand, W. H., & Small, D. M. (1968) *J. Clin. Invest. 47*, 1043−1052.

Ahmed, H. A., Petroni, M. L., Abu-Hamdiyyah, M., Jazrawi, R. P., & Northfield, T. C. (1994) *J. Lipid Res. 35*, 211−219.

Allain, C. A., Poon, L. S., Chan, C. S. G., Richmond, W., & Fu, P. C. (1974) *Clin. Chem. 20*, 470−475.

Almog, S., Kushnir, T., Nir, S., & Lichtenberg, D. (1986) *Biochemistry 25*, 2597−2605.

Almog, S., & Lichtenberg, D. (1988) *Biochemistry 27*, 873−880.

Alonso, A., Sáez, R., Villena, A., & Goñi, F. M. (1982) *J. Membr. Biol. 67*, 55−62.

Armstrong, M. J., & Carey, M. C. (1982) *J. Lipid Res. 23*, 70−80.

Bartlett, G. R. (1959) *J. Biol. Chem. 234*, 466−468.

Bayerl, T. M., Werner, G., & Sackmann, E. (1989) *Biochim. Biophys. Acta 984*, 214−224.

Bentz, J., & Ellens, H. (1988) *Colloids Surf. 30*, 65−112.

Berne, B. J., & Pecora, R. (1976) *Dynamic Light Scattering*, Wiley, New York.

Bourgès, M., Small, D. M., & Dervichian, D. G. (1967a) *Biochim. Biophys. Acta 144*, 157−167.

Bourgès, M., Small, D. M., & Dervichian, D. G. (1967b) *Biochim. Biophys. Acta 144*, 189−201.

Bruckdorfer, K. R., & Sherry, M. K. (1984) *Biochim. Biophys. Acta 769*, 187−196.

Cabral, D. J., & Small, D. M. (1989) *Handbook of Physiology, Section 6: The Gastrointestinal System, Vol. III* (Forte, J. G., & Schultz, S. G., Eds.) pp 621−662, Oxford University Press, Oxford, U.K.

Carey, M. C., & Small, D. M. (1978) *J. Clin. Invest. 61*, 998−1026.

Cohen, D. E., Angelico, M., & Carey, M. C. (1989) *Am. J. Physiol. 257*, G1−G8.

Cohen, D. E., Angelico, M., & Carey, M. C. (1990) *J. Lipid Res. 31*, 55−70.

Cohen, D. E., Leighton, L. S., & Carey, M. C. (1992) *Am. J. Physiol. 263*, G386−G395.

Corradini, S. G., Alvaro, D., Giacomelli, L., Cedola, M., & Angelico, M. (1991) *Biochim. Biophys. Acta 1086*, 125−133.

Donovan, J. M., Jackson, A. A., & Carey, M. C. (1993) *J. Lipid Res. 34*, 1131−1140.

Edwards, K., & Almgren, M. (1992) *Langmuir 8*, 824−832.

Egelhaaf, S. U., & Schurtenberger, P. (1994) *J. Phys. Chem. 98*, 8560−8573.

Ellens, H., Bentz, J., & Szoka, F. C. (1985) *Biochemistry 24*, 3099−3106.

Güldütuna, S., Zimmer, G., Imhof, M., Bhatti, S., You, T., & Leuschner, U. (1993) *Gastroenterology 104*, 1736−1744.

Halpern, Z., Dudley, M. A., Kibe, A., Lynn, M. P., Breuer, A. C., & Holzbach, R. T. (1986) *Gastroenterology 90*, 875−885.

Handbook of Physiology—The Gastrointestinal System III (1989) p 644, Oxford University Press, Oxford, U.K.

Harvey, P. R. C., Sömjen, G., Lichtenberg, M. S., Petrunka, C., Gilat, T., & Strasberg, S. M. (1987) *Biochim. Biophys. Acta 921*, 198−204.

Heuman, D. M., & Bajaj, R. (1994) *Gastroenterology 106*, 1333−1341.

Hjelm, R. P., Thiyagarajan P., & Alkan-Onyuksel, H. (1992) *J. Phys. Chem. 96*, 8653−8661.

Jones, J. D., & Thompson, T. E. (1989) *Biochemistry 28*, 129−134.

Kamp, F., & Hamilton, J. A. (1993) *Biochemistry 32*, 11074−11086.

Kibe, A., Dudley, M. A., Halpern, Z., Lynn, M. P., Breuer, A. C., & Holzbach, R. T. (1985) *J. Lipid Res. 26*, 1102−1111.

Klinkspoor, J. H., Kuver, R., Savard, C. E., Oda, D., Azzouz, H., Tytgat, G. N., Groen, A. K., & Lee, S. P. (1995) *Gastroenterology 109*, 264−274.

Koppel, D. E. (1972) *J. Chem. Phys. 57*, 4814−4820.

Lange, Y., Cohen, C. M., & Poznansky, M. J. (1977) *Proc. Natl. Acad. Sci. U.S.A. 74*, 1538−1542.

Lee, S. P., & Sekijima, J. (1991) *Textbook of Gastroenterology* (Yamada, T., et al., Eds.) pp 1966−1989, J. B. Lippincott Co., Philadelphia.

Lee, S. P., Park, H. Z., Madani, H., & Kaler, E. W. (1987) *Am. J. Physiol 251*, G374−G383.

Lichtenberg, D. (1985) *Biochim. Biophys. Acta 821*, 470−478.

Lichtenberg, D., Robson, R. J., & Dennis, E. A. (1983) *Biochim. Biophys. Acta 737*, 285−304.

Lichtenberg, D., Ragimova, S., Bor, A., Almog, S., Vinkler, C., Peled, Y., & Halpern, Z. (1990) *Hepatology 12*, 149S−154S.

Little, T. E., Lee, S. P., Madani, H., Kaler, E. W., & Chinn, K. (1991) *Am. J. Physiol. 260*, G70−G79.

Liu, C. L., Jain, U. K., Higuchi, W. I., & Mazer, N. A. (1994) *J. Colloid Interface Sci. 162*, 437−453.
Long, M. A., Kaler, E. W., Lee, S. P., & Wignall, G. D. (1994a) *J. Phys. Chem. 98*, 4402−4410.
Long, M. A., Kaler, E. W., & Lee, S. P. (1994b) *Biophys. J.* (in press).
Luk, A. S., Kaler, E. W., & Lee, S. P. (1993) *Biochemistry 32*, 6965−6973.
Luk, A. S., Kaler, E. W., & Lee, S. P. (1996) *Hepatology* (submitted for publication).
Madani, H., & Kaler, E. W. (1990) *Langmuir 6*, 125−132.
Mazer, N. A., & Carey, M. C. (1983) *Biochemistry 22*, 426−442.
Mazer, N. A., Schurtenberger, P., Carey, M. C., Preisig, R., Weigand, K., & Känzig, W. (1984) *Biochemistry 23*, 1994−2005.
McLean, L. R., & Phillips, M. C. (1981) *Biochemistry 20*, 2893−2900.
Nichols, J. W. (1986) *Biochemistry 25*, 4596−4601.
Nichols, J. W., & Ozarowski, J. (1990) *Biochemistry 29*, 4600−4606.
O'Connor, C. J., Wallace, R. G., Iwamoto, K., Taguchi, T., & Sunamoto, J. (1985) *Biochim. Biophys. Acta 817*, 95−102.
Papahadjopoulos, D., Hui, S., Vail, W. J., & Poste, G. (1976) *Biochim. Biophys. Acta 448*, 245−264.
Pedersen, J. S., Egelhaaf, S. U., & Schurtenberger, P. (1995) *J. Phys. Chem. 99*, 1299−1305.
Sagawa, H., Tazuma, S., & Kajiyama, G. (1993) *Am. J. Physiol. 264*, G835−G839.
Salvioli, G., Igimi, H., & Carey, M. C. (1983) *J. Lipid Res. 24*, 701−720.
Schubert, R., & Schmidt, K. (1988) *Biochemistry 27*, 8787−8794.
Schubert, R., Beyer, K., Wolburg, H., & Schmidt, K. (1986) *Biochemistry 25*, 5263−5269.
Schubert, R., Wolburg, H., Schmidt, K., & Roth, H. J. (1991) *Chem. Phys. Lipids 58*, 121−129.
Schurtenberger, P., Mazer, N., & Känzig, W. (1985) *J. Phys. Chem. 89*, 1042−1049.
Schurtenberger, P., Bertani, R., & Känzig, W. (1986) *J. Colloid Interface Sci. 114*, 82−87.
Small, D. M., Bourgès, M. C., & Dervichian, D. G. (1966) *Biochim. Biophys. Acta 125*, 563−580.
Sömjen, G. J., & Gilat, T. (1985) *J. Lipid Res. 26*, 699−704.
Struck, D. K., Hoekstra, D., & Pagano, R. E. (1981) *Biochemistry 20*, 4093−4099.
Tazuma, S., Sasaki, S., Mizuno, S., Sagawa, H., Hashiba, S., Horiuchi, I., & Kajiyama, G. (1989) *Gastroenterology 97*, 173−178.
Thureborn, E. (1966) *Gastroenterology 50*, 775−780.
Ulmius, J., Lindblom, G., Wennerström, H., Johansson, L. B., Fontell, K., Söderman, O., & Arvidson, G. (1982) *Biochemistry 21*, 1553−1560.
Walter, A., Vinson, P. K., Kaplun, A., & Talmon, Y. (1991) *Biophys. J. 60*, 1315−1325.
Yeagle, P. L. (1985) *Biochim. Biophys. Acta 822*, 267−287.

BI962332F